Terra Nova

doi: 10.1111/j.1365-3121.2010.00976.x

Climatic modulation of seismicity in the Alpine–Himalayan mountain ranges

Giuliano F. Panza,[1,2] Antonella Peresan[1,2] and Elisa Zuccolo[1]

[1]*Department of Geosciences, University of Trieste, Via Weiss 4, 34127 Trieste, Italy;* [2]*The Abdus Salam International Centre for Theoretical Physics, ICTP, Strada Costiera 11, 34100 Trieste, Italy*

ABSTRACT

A significant seasonal modulation of seismicity, with a peak in spring and summer, is evidenced in the Himalaya and the Alps, two regions characterized by present day mountain building and glacial retreat. In addition, a secular modulation of seismicity, which can be correlated with surface atmospheric temperature changes in the Northern Hemisphere, is found over the last ten centuries. Therefore, secular variations in permanent glacial dimensions, naturally associated with long-term average surface atmospheric temperature changes, and seasonal snow load may cause crustal deformations that modulate seismicity.

Terra Nova, 23, 19–25, 2011

Introduction

Tectonic forces responsible for mountain building must overcome gravity; this suggests the possibility of competing effects of tectonic forces and the load due to snow and ice cover. Heki (2003) shows that snow load, along the western flank of the backbone range of the Japanese Islands, causes seasonal crustal deformation, perturbs the inter-seismic strain build-up and may seasonally influence seismicity in Japan. Intra-plate earthquakes in northeastern Japan occur on reverse faults, striking parallel to the snow-covered zone, while in central and southwestern Japan, they occur on strike-slip faults, either parallel or perpendicular to the snow cover. The snow load enhances compression at reverse faults, reducing the Coulomb failure stress by a few kPa, a value sufficient to modulate the build-up of tectonic stress (few tens of kPa a^{-1}). The increment in the vertical load in a compressive regime increases the vertical while decreasing the deviatoric stress; consequently, the shear stress remains below the critical value and the faults are more 'stable'. Accordingly, the number of strong earthquakes ($M \geq 7.0$) decreases during snow loading. In regions covered with snow in winter, inland earthquakes tend to be concentrated in spring and summer; however, snow-free regions do not show such behaviour (Heki, 2003). Although the statistical significance of this seasonal correlation is not strong owing to the limited time-span of available observations, it suggests that the spring thaw enhances seismicity beneath the snow cover.

Correspondence: Dr Antonella Peresan, Department of Geosciences, University of Trieste, Via Weiss 4, Trieste 34127, Italy. Tel.: +39 040 5582129; fax: +39 040 5582111; e-mail: aperesan@units.it

We show that the same phenomenology characterizes the continent–continent collision areas of the Himalaya and the Alps, although the main stress field is much more complex than in ocean–continent collision areas, such as Japan.

Ice is about three times denser than snow; therefore, it is reasonable to look for effects of secular variations in glacial extension, which are naturally associated with average global surface atmospheric temperature variations, on the seismicity of mountain ranges.

The areas that can be reliably investigated, in order to validate the presence of the seasonal effect related to spring thaw and to show that a similar phenomenon, but on a very different time-scale (1000 years), is connected with the size variation of permanent glaciers (secular thaw), are located in the Northern Hemisphere. For these regions, the following are available: (i) reliable earthquake catalogues, since at least 1100 (see Table 1); (ii) reports of sizeable variations in permanent glacial extension; and (iii) estimates of average surface atmospheric temperature variations over a sufficiently long period (Esper *et al*., 2002; Hansen *et al*., 2002; Jones and Mann, 2004 and references therein). In the Southern Hemisphere, where estimates of the average surface temperature variation are scarce, the main mountain range (the Andes) essentially strikes N–S, crossing very different climatic zones, and the reported secular thaw is scattered and minor [Barletta, 2007; Dyurgerov and Meier, 2005; GLIMS Glacier Database; World Glacier Inventory (WGI); R-hydroNET v1.0]. Therefore, a quantitative study in the Southern Hemisphere is not warranted.

Data

For the Himalaya, following Heki (2003), earthquakes with $M \geq 7$ are considered. The catalogue is compiled by merging that was used for seismic hazard assessment in India (Parvez *et al*., 2003) with the NOAA–NGDC (1996) data collection, and integrated and revised with information supplied by recent publications. For the Apennines, CPTI04 (Gasperini *et al*., 2004) is used, whereas, for the Alps, the catalogue is compiled by integrating CPTI04 with the data provided by Van Gils and Leydecker (1991). The catalogues are updated using global NEIC (PDE) data, and aftershocks are removed according to Keilis-Borok *et al*. (1980). The frequency–magnitude (FM) distributions for the main shocks in the Alps and Apennines, for different time intervals, are satisfactorily linear for $M \geq 5.3$–5.4, and the overall level of seismic activity increases over time (Fig. 2a,b), in agreement with the analysis performed for the entire Italian territory by Vorobieva and Panza (1993). An optimum magnitude threshold common to seasonal and secular analyses, ensuring sufficient statistics and completeness, is $M \geq 5.7$.

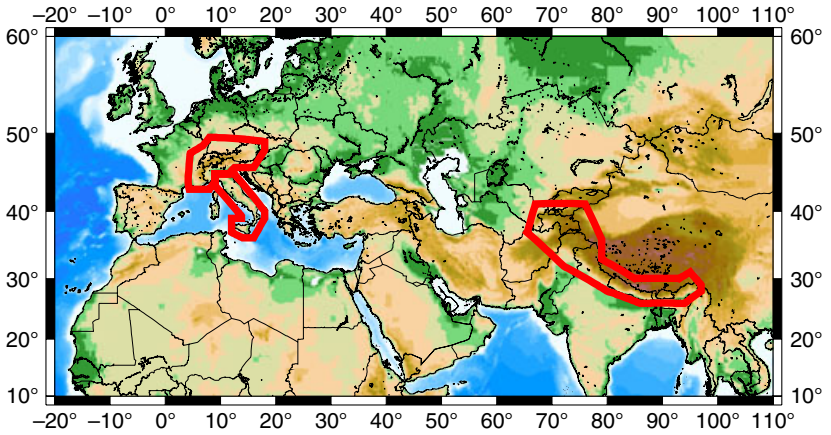

Fig. 1 Polygons defining the three investigated areas: the Alps, the Apennines and the Himalaya.

The earthquake data sources considered are listed in Table 1. For the analysis of seismicity, the catalogues we have compiled are given as Supporting information in Tables S1–S3.

As our source of average surface atmospheric temperature data, we use the data from the study of Esper *et al.* (2002), which are based on tree-ring chronologies (i.e. on the measurements of growth-ring widths in trees; e.g. see http://www.ncdc.noaa.gov/paleo/treering.html) at 14 sites distributed over a large part of the Northern Hemisphere outside the tropics. The tree-ring temperature proxy records preserve coherent large-scale multi-centennial variability at the different sites, thus reflecting temperature changes over the past 1000 years in the Northern Hemisphere.

Seasonal effect

Quantitative analyses of seasonal patterns associated with stress modulation and earthquake occurrence have been published in several papers in the past few years (Gao *et al.*, 2000; Heki, 2003; Saar and Manga, 2003; Christiansen *et al.*, 2005, 2007; Grapenthin *et al.*, 2006; Bollinger *et al.*, 2007; Bettinelli *et al.*, 2008). Snow load, in comparison with other seasonal meteorological phenomena (e.g. rainfall), is characterized by a much longer residence time and a relatively more homogeneous distribution over the surface of the orogen.

As suggested by the theoretical computations of Heki (2003), the seasonal effect is analysed considering only earthquakes that occurred within the crust during the time interval 1850–2008, when for all events, the origin time is specified at least to the day.

As a measure of seismicity, we consider the number of events (N) and the normalized strain (Σ) released by them. Σ is computed using Benioff strain release S_i (Benioff, 1951), calculated for each earthquake i with magnitude M_i, and normalized to the strain $S_{\min}$ of the minimum magnitude $M_{\min}$ considered in the analysis; that is:

$$\Sigma = \sum_i \frac{S_i}{S_{\min}} = \sum_i 10^{\frac{d}{2}(M_i - M_{\min})}, \quad d = \text{const}, \tag{1}$$

where we use the value d = 1.5 given by Gutenberg and Richter (1956).

The earthquakes have been grouped according to the four meteorological seasons: winter (WI: December, January and February), spring (SP: March, April and May), summer (SU: June, July and August) and autumn (AU: September, October and November).

The seasonal (spring–summer) peak is clearly visible in the Himalaya and in the Alps (Fig 3a,b) and corroborates Heki's (2003) findings for Japan. In Fig. 3c,d two counter examples, where the spring–summer peak is not visible, are shown; they represent earthquakes with $M \geq 7.0$ recorded in the period 1900–2008 across the whole Northern Hemisphere (see Fig. 3c; Table 1) and earthquakes in the Apennines with $M \geq 5.7$ recorded in the period 1850–2008 (Fig. 3d). The earthquakes (both N and Σ) in the

Table 1 Earthquake data sources considered in the analysis.

Earthquake data sources			
Region	**Time interval**	**Data source**	**References**
Global	1900–2008	Global Hypocenters' Data Base cd-rom and its updates	NEIC–USGS (1989), Healy *et al.* (1992) and Shebalin (1992, 1997)
	1900–2001	Centennial catalogue	Engdahl and Villaseñor (2002)
Himalaya	25 BC to 2001	Earthquake catalogue of India and surroundings	Parvez *et al.* (2003) and references therein
	2150 BC to 1995	Global Seismicity Catalog cd-rom, 2150 BC to 1995	NOAA–NGDC (1996)
	=	Relevant publications	Feldl and Bilham (2006), Kumar *et al.* (2006), Lave *et al.* (2005), Bilham and Ambraseys (2005) and Pandey and Molnar (1988)
Alps	217 BC to 2001	Parametric catalogue of Italian Earthquakes (CPTI04)	Gasperini *et al.* (2004)
	342 BC to 1990	Historical earthquake catalogues: central and southeastern Europe	Van Gils and Leydecker (1991)
Apennines	217 BC to 2001	CPTI04	Gasperini *et al.* (2004)

Historical information from different regional sources has been cross-checked and integrated. Global datasets are used both for the analysis of seismicity in the Northern Hemisphere and to integrate and update information from regional catalogues.

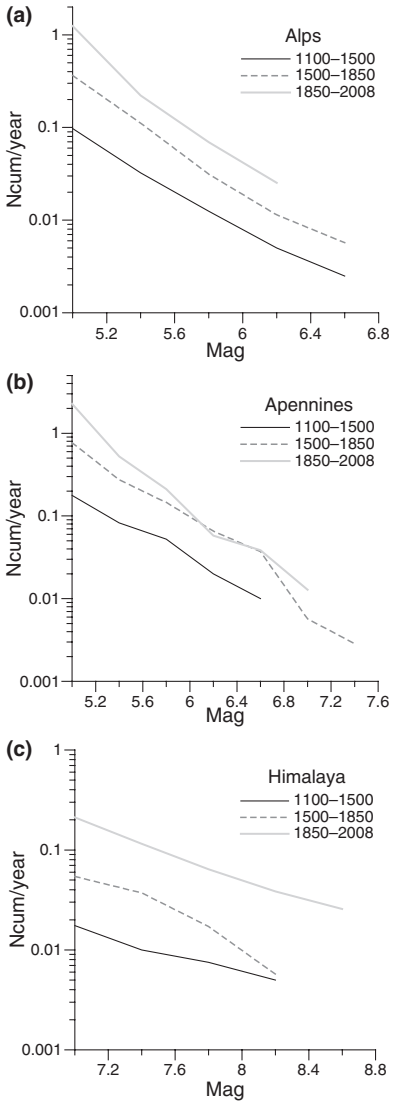

Fig. 2 Cumulative frequency–magnitude distributions for earthquakes (main shocks) that occurred (a) in the Alps, (b) in the Apennines and (c) in the Himalaya (Fig. 1), for the three consecutive time intervals considered for the seasonal and secular analyses.

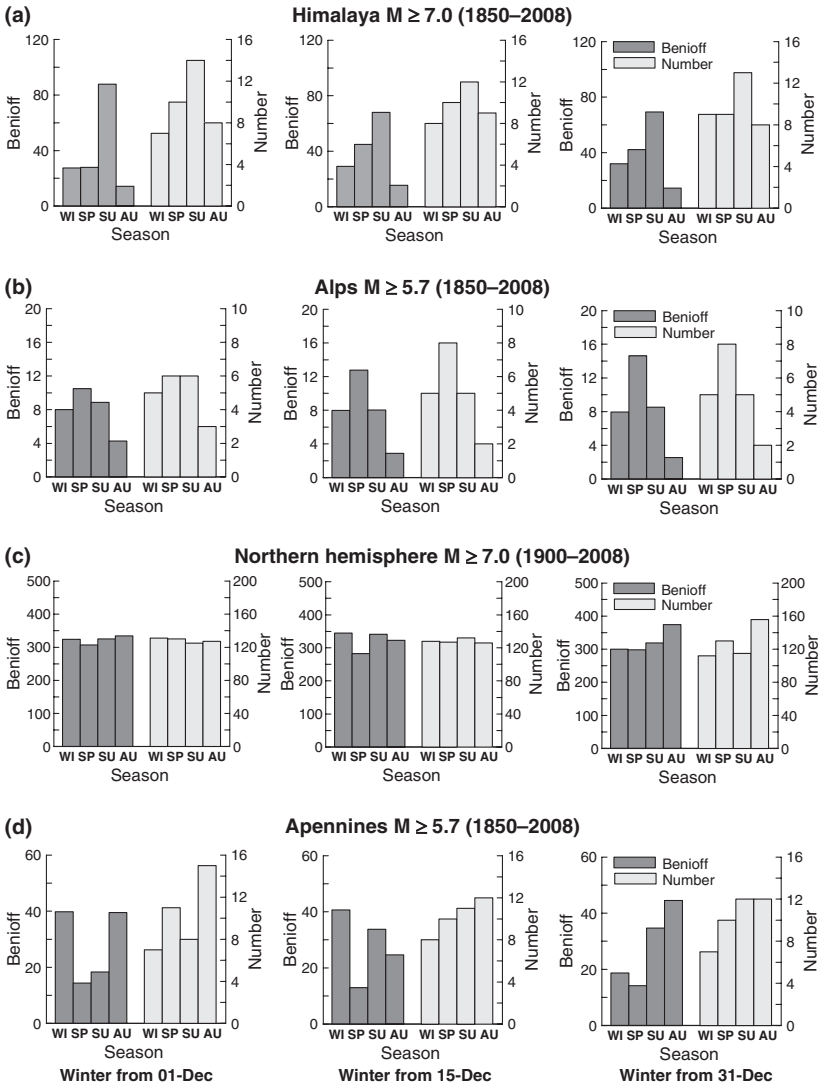

Fig. 3 Histograms of Σ (Benioff) and *N* (Number) for the crustal events that occurred in (a) the Himalayan region, (b) the Alps, (c) the Northern Hemisphere and (d) the Apennines. The three columns correspond to winter starting on 1 December, 15 December and 31 December respectively. For the Northern Hemisphere, if the Alpine and Himalayan events are removed, the flat shape of the histograms remains unchanged. The histograms for two additional intervals (winter starting on 1 November and 15 November respectively) are provided as Supporting information in Figure S1.

whole Northern Hemisphere are distributed rather homogeneously throughout the year, whereas those in the Apennines are concentrated in the winter–autumn.

To account for the variability in the meteorological seasons at different sites, we considered different intervals, shifting the beginning of each season by up to one month (e.g. winter starting on 1, 15 and 31 December respectively, and the remaining seasons being shifted accordingly): the evidenced seasonal effect is very stable (Fig. 3).

A quantitative assessment of the seasonal effect is performed by the classical χ^2 test applied to the number of earthquakes N observed in each season. N is compared with the average number of events expected within a 3-month interval, assuming a uniform distribution of the events over time (Table 2). The χ^2 test shows that the fit to a uniform distribution is appropriate in the Northern Hemisphere, while it can be rejected in the Himalaya and in the Apennines with a confidence level above 90% for N and above 99% for Σ. The deviation from a uniform distribution in the Apennines, where the snow load effect is not significant, is due to a significant peak of seismicity in the winter season. In the Alps, owing to the relatively small number of earthquakes with $M \geq 5.7$, the uniform distribution for N cannot be rejected, while the difference turns out to be

Table 2 χ^2 test statistic obtained by comparing the seasonal seismicity distribution (Σ and N) shown in Fig. 3 with a uniform distribution.

χ^2 test statistic for seasonal distributions		
Region	Σ	N
Himalaya	93.84 (<0.01)	2.95 (0.08)
Alps	2.98 (0.08)	1.20 (0.27)
Northern Hemisphere	1.21 (0.27)	0.18 (0.67)
Apennines	19.98 (<0.01)	3.78 (0.05)

The test is performed with d.f. = 1 degrees of freedom (four classes). The *P*-value is given in parentheses; low values of *P* indicate a poor fit to the uniform distribution. The values reported in the table were obtained for winter starting on 1 December; similar values apply to different seasonal groupings.

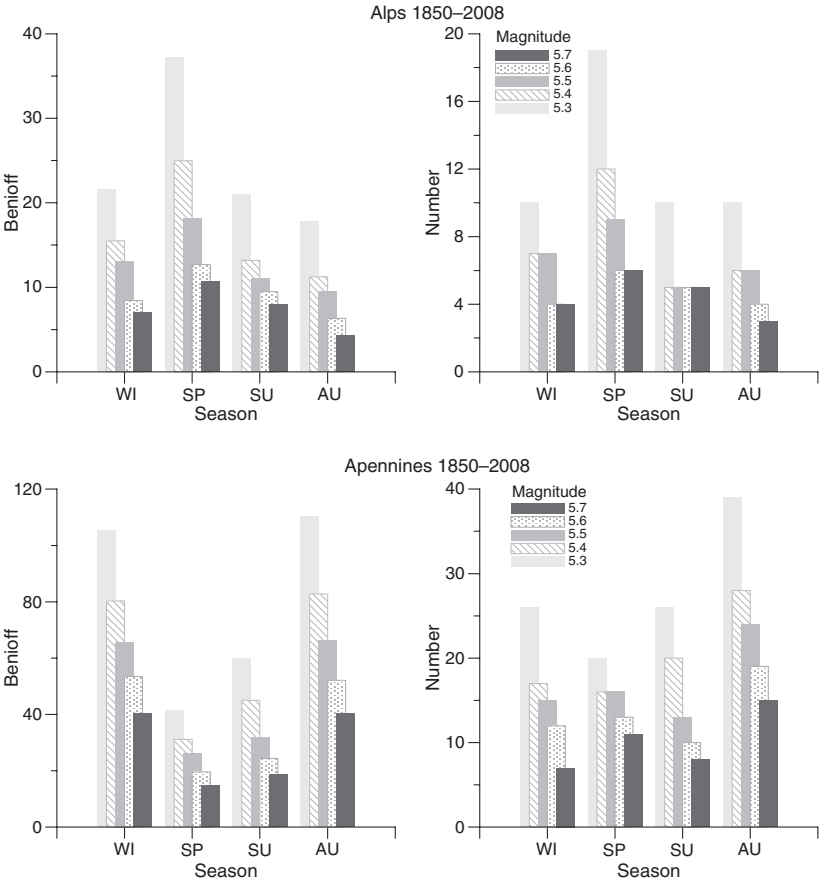

Fig. 4 Histograms of Σ and N for the crustal events that occurred in 1850–2008, in the Alps and in the Apennines. Five magnitude thresholds are considered, from 5.7 down to 5.3. The shapes of the histograms remain very stable, especially when Σ is considered. The deviation from a uniform distribution is significant for $M = 5.3$, both for Σ (Alps: $\chi^2 = 6.20$, $P = 0.01$; Apennines: $\chi^2 = 45.2$, $P < 0.01$) and for N (Alps: $\chi^2 = 2.82$, $P = 0.09$; Apennines: $\chi^2 = 7.53$, $P < 0.01$).

significant at the 90% confidence level for Σ. In the Alps and Apennines, where the catalogue is certainly complete down to magnitude 5.3 since 1850, the statistical significance of the test improves when a lower magnitude threshold is considered; the observed seasonal pattern is clearly visible and stable with respect to variations in M (Fig. 4), especially when strain release Σ is considered.

The seasonal effect found in the Apennines may be explained by a mechanism similar to that proposed in a recent local study of Nepalese seismicity by Bollinger *et al*. (2007) for the period 1995–2000. During this period, only moderate earthquakes ($M \leq 6.3$) have been recorded, and a marked reduction in the number of events (N) is observed in summer. This phenomenon is attributed to the stress loading accompanying monsoon rains in the Ganges and northern India.

Our findings, based on both N and Σ, show that on a much longer time series and along the whole Himalaya chain, in spite of the monsoon rains effect, there is a clear spring–summer seasonal peak in seismicity with $M \geq 7.0$. Thus, the reduction in seismicity in summer seems to be limited to the number N of moderate events ($M \leq 6.3$), which mostly occur in the upper crust, whose contribution to the seismic strain release Σ is minor compared with that of the necessarily deeper $M \geq 7.0$ crustal events, which are modulated by the snow load. In fact, snow and monsoon induce similar sized stress variations and have the same periodicity (e.g. Heki, 2003; Bettinelli *et al*., 2008), but different spatial extensions and residence times. Snow load is distributed on the Earth's surface and affects the whole chain rather homogeneously, while the rain load from the monsoon is more scattered within the various drainage basins and water storage depositories in the uppermost crust.

Fluid diffusion should have relatively modest effects at large depths, implying depth dependent seismic triggering. Depth determinations, however, are not available with the necessary precision or do not exist at all in the considered periods of time; therefore, the effect of fluids compared with that of ice and snow cannot be sorted out by assessing the depth dependence of the seasonal modulation. If the analysis is limited to the period for which statistically sufficient data are available, i.e. to the last fifty years, the seasonal distributions of moderate and large earthquakes in the Apennines turn out to be depth-independent.

Secular effect

The histograms of Σ and N vs. time in the Alps and Himalaya and the average surface atmospheric temperature variations over the past millennium in the Northern Hemisphere, expressed as an index value inferred from tree-ring records (Esper *et al*., 2002), are reported in Fig. 5. The histograms point towards the existence of a secular modulation of seismicity due to size variations of the permanent glaciers, as mirrored by the average surface atmospheric temperature variations.

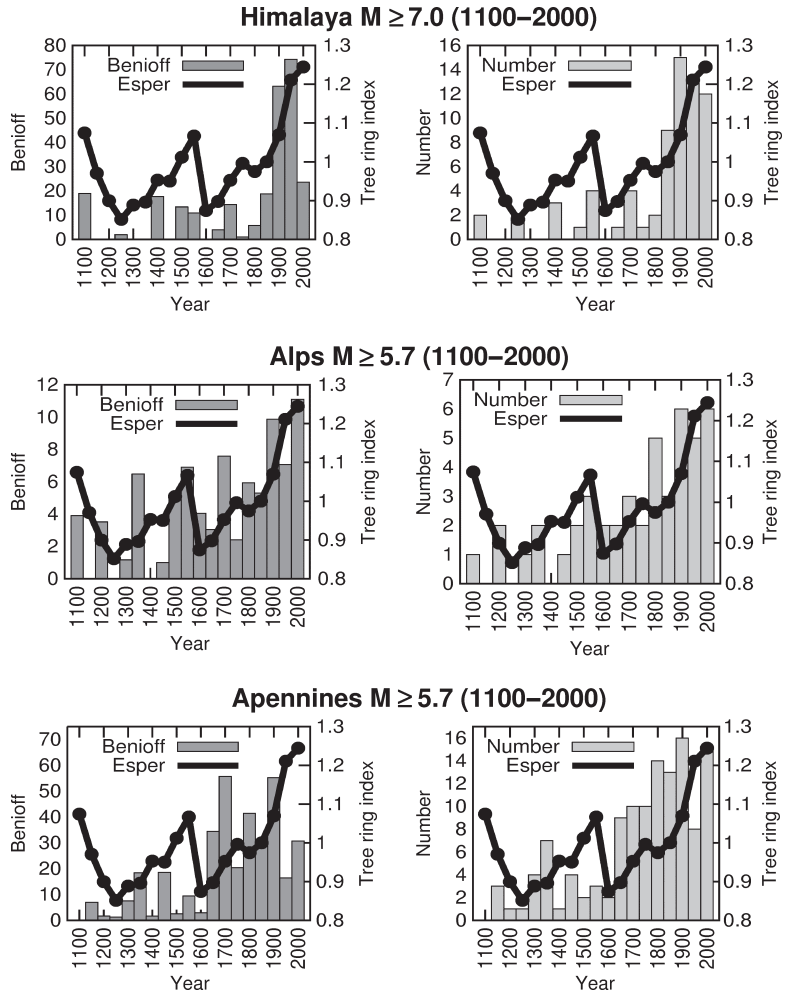

Fig. 5 Histograms showing Σ and N, in 50-year bins for the considered areas, and average surface atmospheric temperature. A quantitative estimate of the statistical significance of the correlation between seismicity and temperature variation is given in Table 3.

A suitable (counter) example, capable of addressing questions about the possible lack of completeness in the catalogues before 1850 for events of a size relevant to our analysis, is supplied by the seismicity recorded in the Apennines. There, the melting of perennial glaciers, due to global warming, is negligible [Dyurgerov and Meier, 2005; GLIMS Glacier Database; World Glacier Inventory (WGI)], and the seismicity (N and Σ) remains almost constant or, in the last century, even decreases. Although we cannot exclude the possibility that the increase in seismicity rate in the last three centuries, reported by Caputo (2000) and Vorobieva and Panza (1993) and clearly visible in Fig. 5, can be related to improved earthquake detection, the catalogue completeness threshold for the Alps and Apennines (Fig. 2) is M = 5.3–5.4 for the period 1100–1850, which is well below the M = 5.7 considered for our analysis.

Owing to the limited amount and type of data, a very suitable tool for statistical analysis of the correlation between average surface atmospheric temperature (Esper *et al.*, 2002) and seismicity (N and Σ) is Spearman's rank correlation coefficient (Spearman, 1904), which is a robust and resistant nonparametric measure of correlation. It assesses how well an arbitrary function (not necessarily linear) describes the relationship between two variables, with no assumptions about the frequency distributions of the variables.

Spearman's rank correlation coefficient, r_{rank}, is computed as follows:

$$r_{\text{rank}} = 1 - \frac{6\sum d_i^2}{n(n^2-1)}, \quad i = 1, n, \quad (2)$$

where d_i is the difference in rank between the ith pair of data values in the two datasets.

The correlation coefficients, computed using time bins of 50 years, are given in Table 3 and corrected for tied ranks according to Siegel and Castellan (1988).

From the results summarized in Table 3, the statistical significance of the correlation between changes in average surface atmospheric temperature and seismic activity (N and Σ) is evident in the Alps and Himalaya, while in the Apennines, where glaciation and subsequent glacial shrinking have been minor over the past millennium, the correlation is certainly missing. The use of Spearman's test, even when applied to a small dataset such as the Alps, shows features that could be missed by a simple visual inspection of the data.

Our findings generalize to different seismotectonic regions and to long time-scales the observations made about the effect of deglaciation on magmatism (Jull and McKenzie, 1996) and recent seismicity in volcanic areas (Pagli and Sigmundsson, 2008).

Table 3 Spearman's correlation coefficient between seismicity (Σ and N) and average surface atmospheric temperature estimated for different time intervals.

Spearman's correlation coefficients				
Region	**Σ since 1100**	***N* since 1100**	**Σ since 1500**	***N* since 1500**
Himalaya	0.79 (<0.01)	0.69 (<0.01)	0.79 (0.01)	0.78 (0.01)
Alps	0.56 (0.01)	0.56 (0.01)	0.65 (0.03)	0.68 (0.02)
Apennines	0.20 (0.41)	0.34 (0.16)	−0.14 (0.69)	0.32 (0.34)

The confidence level is ≥95% (P-value, given in parentheses, is ≤0.05) in the Alps and Himalaya. The strength of the Spearman's test, even when applied to a small dataset, is evident when comparing the results of the Alps and the Apennines, which are much more different from that one would expect from a simple visual inspection of the data.

Conclusion

The seasonal (spring–summer) peak in the seismicity recorded in the Alps and Himalaya since 1850 confirms Heki's (2003) findings for Japan, thus adding statistical significance to the spring thaw enhancement of seismicity beneath snow cover.

The mini-glaciation from about 1350 to about 1850, well documented in the Northern Hemisphere (Esper *et al*., 2002; Jones and Mann, 2004 and references therein; Imbrie and Imbrie, 1979), correlates well with a low level of seismicity. Seismic activity increases very rapidly after 1850, in correspondence with the beginning of the ongoing warm period (Esper *et al*., 2002; Jones and Mann, 2004; Ward, 2009 and references therein).

We can thus conclude that secular and seasonal thaw may cause crustal deformations that modulate seismicity in the active mountain ranges of the Alps and Himalaya.

Acknowledgements

We acknowledge useful discussions with V. Kossobokov, B. N. Upreti, M. Caputo and D. Anderson. This research was partly developed in the framework of the project 'Giovani Ricercatori', funded by the University of Trieste, and of the ASI – Pilot Project 'SISMA: SISMA – Information System for Monitoring and Alert'. The study benefited from funding provided by the Italian Presidenza del Consiglio dei Ministri – Dipartimento della Protezione Civile (DPC); scientific papers funded by DPC do not represent its official opinion and policies.

References

Barletta, V.R., 2007. *New Constraints on Mantle Viscosity and ice Mass Variations Inferred From Combined Satellite and Ground Data*. Fig. n. 5.21, PhD thesis, University of Milano, XX Ciclo.

Benioff, H., 1951. Earthquakes and rock creep. *Bull. Seism. Soc. Am*., **41**, 31–69.

Bettinelli, P., Avouac, J.-P., Flouzat, M., Bollinger, L., Ramillien, G., Rajaure, S. and Sapkota, S., 2008. Seasonal variations of seismicity and geodetic strain in the Himalaya induced by surface hydrology. *Earth Planet. Sci. Lett*., **266**, 332–344.

Bilham, R. and Ambraseys, N., 2005. Apparent Himalayan slip deficit from the summation of seismic moments for Himalayan earthquakes, 1500–2000. *Curr. Sci*., **88**, 1658–1663.

Bollinger, L., Perrier, F., Avouac, J.P., Sapkota, S., Gautam, U. and Tiwari, D.R., 2007. Seasonal modulation of seismicity in the Himalaya of Nepal. *Geophys. Res. Lett*., **34**, L08304, doi: 10.1029/2006GL029192.

Caputo, M., 2000. Comparison of five independent catalogues of earthquakes of a seismic region. *Geophys. J. Int*., **143**, 417–426.

Christiansen, L.B., Hurwitz, S., Saar, M.O., Ingebritsen, S.E. and Hsieh, P.A., 2005. Seasonal seismicity at western United States volcanic centers. *Earth Planet. Sci. Lett*., **240**, 307–321.

Christiansen, L.B., Hurwitz, S. and Ingebritsen, S., 2007. Annual modulation of seismicity along the San Andreas Fault near Parkfield, CA. *Geophys. Res. Lett*., **34**, L04306, doi:10.1029/2006GL028634.

Dyurgerov, M.B. and Meier, M.F., 2005. *Glaciers and the Changing Earth System: A 2004 Snapshot*. Occasional Paper 58, Institute of Arctic and Alpine Research, University of Colorado, Boulder, Colorado, 117 p. Available at: http://instaar.colorado.edu/other/occ_papers.html.

Engdahl, E.R. and Villaseñor, A., 2002. Global Seismicity: 1900–1999. In: *International Handbook of Earthquake and Engineering Seismology* (W.H.K. Lee, H. Kanamori, P.C. Jennings and C. Kisslinger, eds), Part A, Chapter 41, pp. 665–690, Boston: Academic Press.

Esper, J., Cook, E.R. and Schweingruber, F.H., 2002. Low-frequency signals in long tree-ring chronologies for reconstructing past temperature variability. *Science*, **295**, 5563.

Feldl, N. and Bilham, R., 2006. Great Himalayan earthquakes and the Tibetan plateau. *Nature*, **444**, 165–170, doi: 10.1038/nature05199.

Gao, S.S., Silver, P.G., Llnde, A.T. and Sacks, I.S., 2000. Annual modulation of triggered seismicity following the 1992 Landers earthquake in California. *Nature*, **406**, 500–504.

Gasperini, P., Camassi, R., Mirto, C. and Stucchi, M., 2004. *Catalogo Parametrico dei Terremoti Italiani, Versione 2004 (CPTI04)*. INGV, Bologna. Available at: http://emidius.mi.ingv.it/CPTI04/.

GLIMS Glacier Database. National Snow and Ice Data Center, Cooperative Institute for Research in Environmental Sciences at the University of Colorado at Boulder. http://glims.colorado.edu/glacierdata/

Grapenthin, R., Sigmundsson, F., Geirsson, H., Árnadóttir, T. and Pinel, V., 2006. Icelandic rhythmics: annual modulation of land elevation and plate spreading by snow load. *Geophys. Res. Lett*., **33**, L24305.

Gutenberg, B. and Richter, C.F., 1956. Earthquake magnitude, intensity, energy and acceleration. *Bull. Seism. Soc. Am*., **46**, 105–145.

Hansen, J., Ruedy, R., Sato, M. and Lo, K., 2002. Global warming continues. *Science*, **295**, 275, doi: 10.1126/science.295.5553.275c.

Healy, J.H., Kossobokov, V.G. and Dewey, J.W.1992. *A Test to Evaluate the Earthquake Prediction Algorithm, M8*. U.S. Geological Survey Open-File Report 92-401, 23 p. with 6 Appendices.

Heki, K., 2003. Snow load and seasonal variation of earthquake occurrence in Japan. *Earth Planet. Sci. Lett*., **207**, 159–164.

Imbrie, J. and Imbrie, K. P., 1979. *Ice Ages*. Enslow Publishers, Hillside, New Jersey.

Jones, P. D. and Mann, M. E., 2004. Climate over past millennia. *Rev. Geophys*., **42**, RG2002, doi: 10.1029/2003RG000143.

Jull, M. and McKenzie, D., 1996. The effect of deglaciation on mantle melting beneath Iceland. *J. Geophys. Res*., **101**, 21815–21821.

Keilis-Borok, V.I., Knopoff, L. and Rotwain, I.M., 1980. Burst of aftershocks, long-term precursors of strong earthquakes. *Nature*, **283**, 259–263.

Kumar, S., Wesnousky, S.G., Rockwell, T.K., Briggs, R.W., Thakur, V.C. and Jayangondaperumal, R., 2006. Paleoseismic evidence of great surface rupture earthquakes along the Indian Himalaya. *J. Geophys. Res*., **111**, B03304, doi: 10.1029/2004JB003309.

Lave, J., Yule, D., Sapkota, S., Bassant, K., Madden, C., Attal, M. and Pandey, R., 2005. Evidence for a great medieval earthquake (–1100 AD) in the Central Himalayas. *Nepal Sci*., **307**, 1302–1305.

NEIC–USGS, 1989. *Global Hypocenters*' Data Base. CD-ROM, NEIC/USGS, Denver.

NOAA–NGDC, 1996. *The Seismicity Catalog CD-ROM Collection. Volume 2*. NOAA's National Geophysical Data Center Available at: http://www.ngdc.noaa.gov/hazard/data/cdroms/Seismicity_v2/data/asia/.

Pagli, C. and Sigmundsson, F., 2008. Will present day glacier retreat increase volcanic activity? Stress induced by recent glacier retreat and its effect on magmatism at the Vatnajokull ice cap, Iceland. *Geophys. Res. Lett*., **35**, L09304, doi:10.1029/2008GL033510.

Pandey, M. R. and Molnar, P., 1988. The distribution of Intensity of the Bihar Nepal earthquake of 15 January 1934 and bounds on the extent of the rupture. *J. Nepal Geol. Soc*., **5**, 22–44.

Parvez, I. A., Vaccari, F. and Panza, G.F, 2003. A deterministic seismic hazard map of India and adjacent areas. *Geophys. J. Int*., **155**, 489–508.

R-hydroNET v1.0. *A Regional, Electronic Hydrometeorological Data Network for South America, Central America, And The Caribbean*, (C.J. Vörösmarty, C. Fernandez-Jauregui and M.C. Donosa, eds). Available at: http://www.rhydronet.sr.unh.edu/grids/precipitation/sa.html.

Saar, M.O. and Manga, M., 2003. Seismicity induced by seasonal groundwater recharge at Mt. Hood, Oregon. *Earth Planet. Sci. Lett.*, **214**, 605–618.

Shebalin, P.N., 1992. *Automatic Duplicate Identification in Set of Earthquake Catalogues Merged Together*. U.S. Geological Survey Open-File Report 92-401, Appendix II.

Shebalin, P.N., 1997. User manual for UPDATE. In: *Algorithms for Earthquake Statistics and Prediction* (J.H. Healy, V.I. Keilis-Borok and W.H.K. Lee, eds). *Seismol. Soc. Am*, **6**, 167–221. IASPEI Software Library, El Cerrito, CA.

Siegel, S. and Castellan Jr, N.J., 1988. *Nonparametric Statistics for the Behavioral Sciences*, 2nd edn. Wiley, New York, 285 p.

Spearman, C., 1904. The proof and measurement of association between two things. *Am. J. Psychol.*, **15**, 72–101.

Van Gils, J.M. and Leydecker, G. (eds), 1991. *Catalogue of European Earthquakes With Intensities Higher Than 4*. Commission of the European Communities – nuclear science and technology, Brussels, Luxembourg, 353 pp.

Vorobieva, I. and Panza, G.F., 1993. Prediction of the occurrence of related strong earthquakes in Italy. *PAGEOPH*, **141**, 25–41.

Ward, P.L., 2009. Sulfur dioxide initiates global climate change in four ways. *Thin Solid Films*, **47**, 3188–3203.

World Glacier Inventory (WGI) - National Snow and Ice Data Center. NOAA Environmental Services Data and Information Management (ESDIM). Available at http://nsidc.org/data/glacier_inventory/index.html.

Received 6 February 2010; revised version accepted 13 September 2010

Supporting information

Additional Supporting Information may be found in the online version of this article:

Figure S1. Histograms of Σ (Benioff) and *N* (Number) for the crustal events that occurred in (a) the Himalayan region, (b) the Alps, (c) the Northern Hemisphere and (d) the Apennines.

Figure S2. Histograms of Σ (Benioff) and *N* (Number) for the crustal events, which occurred in the Apennines in the period 1950–2008 (winter starting on 1 December).

Table S1. List of the earthquakes that occurred in the Himalaya in the time interval 1100–2008.

Table S2. List of the earthquakes that occurred in the Alps in the time interval 1100–2008.

Table S3. List of the earthquakes that occurred in the Apennines in the time interval 1100–2008.

Please note: Wiley-Blackwell are not responsible for the content or functionality of any supporting materials supplied by the authors. Any queries (other than missing material) should be directed to the corresponding author for the article.

